Building and Environment 233 (2023) 110088

Contents lists available at ScienceDirect

Building and Environment

journal homepage: www.elsevier.com/locate/buildenv

Dynamic behavior of gas-phase NCl_3 and CO_2 in indoor pool facilities

Lester T. Lee [a], Tianren Wu [a,b], Brandon E. Boor [a,b], Ernest R. Blatchley III [a,c,*]

[a] Lyles School of Civil Engineering, Purdue University, West Lafayette, IN, USA
[b] Ray W. Herrick Laboratories, Center for High Performance Buildings, Purdue University, West Lafayette, IN, USA
[c] Division of Environmental and Ecological Engineering, Purdue University, West Lafayette, IN, USA

ARTICLE INFO

Keywords:
Indoor air quality
Swimming pool chemistry
Volatile disinfection byproducts
Trichloramine
Two-film theory

ABSTRACT

The presence of gas-phase trichloramine (NCl_3) in indoor swimming pool facilities is associated with adverse health outcomes among swimmers and other pool users, as well as degradation of pool infrastructure. Given their similarities in terms of volatility (*i.e.*, Henry's law constant), the dynamic behaviors of NCl_3 and carbon dioxide (CO_2) in the air above indoor pools were postulated to be similar. Experiments were conducted to characterize and quantify the dynamic behavior of gas-phase NCl_3 and CO_2 in a mechanically ventilated swimming pool facility. The results of these time-course measurements allowed for examination of the effects of background water circulation and swimmer-induced mixing on the dynamics of both compounds in the air space above an indoor swimming pool. Measured gas-phase NCl_3 concentrations exceeded the suggested guideline values of 300 $\mu g/m^3$ or 500 $\mu g/m^3$ during periods of heavy use. Measured gas-phase CO_2 concentration followed a similar dynamic pattern as gas-phase NCl_3; gas-phase CO_2 concentrations often exceeded 1000 ppm_v during swimming meets. Mass balance models for gas-phase NCl_3 and CO_2 were developed to relate the characteristics of the indoor pool environment to their dynamics. The results of these modeling efforts indicated that the similarity of CO_2 transfer behavior to NCl_3 may allow the use of CO_2, which can be measured with low-cost infrared gas sensors, as a control parameter for NCl_3. Moreover, the models that were developed to describe the dynamic behaviors of these volatile compounds may serve as tools for pool design, optimization of pool operations, and control of their mechanical ventilation systems.

1. Introduction

Swimming is a common activity that can yield numerous health benefits, including reductions in blood pressure, as well as the risks of heart disease, diabetes, and stroke [1]. Swimming has become a year-around activity in temperate and cold regions due to the construction of indoor swimming pools. Swimming pool water must undergo treatment to achieve safe, clear water and to eliminate harmful substances, including waterborne microbial pathogens. Most swimming pool water treatment systems are based on water recirculation through filtration and chlorine-based disinfection, although other treatment processes are often used to complement these methods [2], including ultraviolet (UV) irradiation to promote disinfection and contaminant oxidation, secondary oxidants to complement chlorination, or coagulant chemicals to improve filtration.

Chlorine reacts with various organic and inorganic compounds to produce disinfection byproducts (DBPs) in swimming pools. Notable precursors to DBP formation in pools include organic-N compounds, such as urea, uric acid, creatinine, and amino acids [3–11]. Among the DBPs produced by these reactions are the inorganic chloramines. Transfer of trichloramine (NCl_3) and other volatile compounds from swimming pool water to air offers the potential for human exposure to these chemicals through respiration [12]; dermal uptake and ingestion represent pathways for exposure for some other DBPs [13].

The effects of human exposure to gas-phase NCl_3 have been examined extensively due to its association with irritation of the respiratory systems of swimmers and pool patrons in chlorinated, indoor swimming pool facilities [14–17]. NCl_3 is particularly volatile compared with other volatile DBPs that are common to pools, including the other inorganic chloramines (monochloramine (NH_2Cl) and dichloramine ($NHCl_2$)) [18]. Gas-phase NCl_3 is largely responsible for the chlorine odor in indoor swimming pool facilities and has been linked to corrosion of metal surfaces in these facilities [19]. NCl_3 can irritate the eyes, skin, and the respiratory system [17,20,21]. Several studies have shown positive correlations between irritation symptoms among swimmers and pool workers with high gas-phase NCl_3 concentrations at indoor pool

* Corresponding author. Lyles School of Civil Engineering, Purdue University, 550 Stadium Mall Drive, West Lafayette, IN, 47907, USA.
E-mail address: blatch@purdue.edu (E.R. Blatchley).

https://doi.org/10.1016/j.buildenv.2023.110088
Received 5 November 2022; Received in revised form 3 February 2023; Accepted 7 February 2023
Available online 13 February 2023
0360-1323/© 2023 Elsevier Ltd. All rights reserved.

facilities [22,23]. Long-term studies of gas-phase NCl_3 concentration in indoor chlorinated swimming pools have been conducted in recent years [24–27].

The quality of indoor air in swimming pool facilities is strongly linked to the formation and presence of volatile DBPs in swimming pool water. Two-film theory suggests that the conditions that lead to net liquid→gas phase transfer of NCl_3 will also lead to net liquid→gas phase transfer of other volatile compounds that are present in swimming pool water. As such, gas-phase NCl_3 could serve as a sentinel compound for indoor air quality (IAQ) in pool facilities.

IAQ in swimming pool facilities is known to be affected by many factors, including: bather load, the hygiene habits of swimmers, water treatment processes, and heating, ventilation, and air conditioning (HVAC) system characteristics [24,28–30]. At present, the effects of these factors on IAQ are understood only at an empirical, qualitative level. The lack of a quantitative understanding of the effects of these factors on IAQ makes it difficult to design and implement measures to improve air quality in indoor swimming pool facilities.

Carbon dioxide (CO_2) is another volatile compound that is present in pool water. CO_2 is similar to NCl_3 in terms of its volatility, as indicated by their respective Henry's law constants. CO_2 is also easier and less expensive to measure in the gas and liquid phases than NCl_3. As such, CO_2 may represent a surrogate for NCl_3 and other volatile DBPs that are common to swimming pool water [31]. However, the gas-phase concentration of CO_2 may also be influenced by other processes, notably including human respiration, which may complicate the use of CO_2 as a proxy for NCl_3.

In this study, the gas-phase concentrations of NCl_3 and CO_2 were monitored over extended periods in a mechanically ventilated indoor swimming pool facility. In addition, liquid-phase concentrations of NCl_3, CO_2, and several relevant water quality parameters were measured. Basic operational characteristics of the HVAC system were also recorded at the pool facility. Measurements were conducted over a range of use conditions, including periods of non-use, periods of typical use, and periods of heavy use, when water and air quality were expected to be poorest.

Mass balance-based models were developed to describe the dynamic behavior of IAQ, as defined by the gas-phase concentrations of NCl_3 and CO_2 in the swimming pool facility. The governing equations were developed to include terms to quantify the effects of the factors that are known to affect IAQ in mechanically ventilated indoor pool facilities.

2. Materials and methods

2.1. Study site: indoor aquatic center

Measurements were conducted at an indoor pool facility. The facility includes two main water bodies: a competition pool with dimensions of 25-yards (22.9 m) wide x 50-m long, with an average depth of 8.2 ft (2.5 m) and a diving well with dimensions of 20-yards (18.3 m) wide, 25-yards (22.9 m) long, and 17 ft (5.2 m) deep. The two water bodies are hydraulically independent, and each has its own water treatment/recirculation system. The treatment systems for both pools include a high-rate sand filter, UV disinfection (based on medium-pressure Hg lamps), pH control by addition of CO_2 gas and/or muriatic acid (HCl), and an erosion chemical feeder for addition of calcium hypochlorite. A moveable bulkhead divides the competition pool into two sides. During short-course swimming meets (competitions in pools with length of 25-yd or 25-m), one side of the competition pool is used as the 'competition side' where actual swimming races are held, while the other side is used for warm-up/warm-down activities. Water samples were collected from the same location in all experiments. Schematic illustrations of the layout of the pool facility, including the locations of water sample and air monitoring equipment are presented in Figures SI-1, SI-2, and SI-3.

The facility includes five air handlers that are designed to introduce fresh (outdoor) air and recirculate indoor air; however, it should be noted that recirculated air will not affect indoor air quality, as described by the IAQ models presented herein. The volumetric rate of outdoor air introduction was assumed to be equal to the volumetric rate of air exhaust from the facility. The volumetric rate of air introduction to the facility is normally held at a constant value. However, the air flow rate is sometimes altered to allow cooling when outside air is cooler than the indoor thermostat setting. Also, outdoor air flow rates through the air handlers are sometimes increased to reduce gas-phase NCl_3 concentration. Each of the five air handlers is capable of delivering outdoor air at a volumetric flow rate up to approximately 25,000 ft^3/min (*ca.* 42,000 m^3/h). The total air volume within the natatorium is roughly 1.84×10^6 ft [3] (52,100 m^3).

Water samples were collected at the studied pool before and during swimming meets that were held at the facility. Sample collection was also conducted during regular pool operating hours (6 a.m.–10 p.m.). Pool water samples were collected periodically depending on swimming meet schedules and times when the pool was open to the public. Water samples were collected from a fixed position in the pool at a depth of 30 cm from the surface; samples were collected in 50 mL terephthalate bottles with screw caps. Water samples were collected with essentially zero headspace to minimize losses due to liquid→gas transfer. Samples were transported to the laboratory as soon as possible after collection for analysis, usually within 2 h of sample collection.

2.2. Experimental design

Three sets of experiments were conducted throughout this study. Time-course monitoring of liquid and gas-phase NCl_3 was conducted in experiments A and B. Time-course monitoring of liquid and gas-phase CO_2 was conducted in experiments B and C. Tables 1 and 2 provide summaries of the operating conditions of the pool during each of the experiments, including age of swimmers, type of swimmers, and type of pool operation. Also, the instruments and measurements that were applied in each of the experiment sets are defined in these tables.

2.3. Liquid- and gas-phase NCl_3 measurements

Liquid-phase concentrations of NCl_3 were measured by Membrane Introduction Mass Spectrometry (MIMS). The MIMS system used in this study comprised an Agilent GC-MS system (5975C mass-selective detector (MSD) and 6850 gas chromatograph (GC)) with a membrane injection device. The GC was used only for temperature control of the membrane interface (*i.e.*, no chromatography was used). The system was operated with electron ionization (70 eV). NCl_3 was identified using mass spectrum scan mode ($49 \leq m/z \leq 200$) and further quantified with selected ion monitoring (SIM). Liquid-phase NCl_3 concentration was estimated based on ion abundance at m/z of 119 amu.

Measurements of gas-phase NCl_3 concentration were conducted using Next Environmental Monitoring (NEMo) IAQ monitors (Ethera Labs, Crolles, France, model NEMo XT). Previous studies have demonstrated the application of NEMo devices in indoor swimming pool facility environments [24,29]. The NEMo devices provide near real-time measurements of gas-phase NCl_3 at the ppb_v level. Measurements of gas-phase NCl_3 concentrations by the NEMo device are based on the colorimetric signal that develops from the reaction between NCl_3 and potassium iodide (KI); the measurements are reported as a 30-min moving average, reported every 10 min. Further details of the configuration of NEMo device and operational limitations have been presented previously [24]. The NEMo devices were mounted on a wall of the studied indoor facility. The devices were positioned roughly 4 m laterally and 4.5 m above the edge of the pool water surface (see Figures SI-1, SI-2, and SI-3).

Table 1
Summary of conditions for experiments A and B and corresponding estimates of mass transfer coefficients for NCl_3.

Experiment	Pool operation	Type of swimmer	Age of swimmers	Measurements	Instruments	K_l (m/hour)	K_lA (m^3/hour)	K' (m^3/hour)
A	Normal operations	Daily lap swimmers and swim team practice	Adults and college students	Gas-phase and liquid-phase NCl_3	MIMS NEMo	0.0024	4.07	5.40
B	Swimming meet	Age group swimmers	8 and under	Gas-phase and Liquid-phase NCl_3	MIMS NEMo	0.0022	3.67	0.80

Table 2
Summary of conditions for experiments B and C and corresponding estimates of mass transfer coefficients for CO_2.

Experiment	Pool operation	Type of swimmer	Age of swimmers	Measurements	Instruments	K_l (m/hour)	K_lA (m^3/hour)	K' (m^3/hour)
B	Swimming meet	Age group swimmers	8 and under	Water pH, alkalinity, and temperature; gas-phase CO_2	NEMo	0.045	75.2	0
C	Swimming meet	Collegiate athletic	College students	Water pH, alkalinity, and temperature; gas-phase CO_2	LI-COR CO_2 analyzer	0.051	85.2	10

2.4. Liquid- and gas-phase CO_2 measurements

Gas-phase CO_2 concentrations were monitored using the NEMo devices for experiment B; the NEMo devices are equipped with a nondispersive infrared gas sensor in its chamber. For experiment C, gas-phase CO_2 concentrations were monitored using a LI-830 CO_2 gas analyzer (LI-COR Biosciences, Lincoln, Nebraska). Liquid-phase CO_2 concentrations were calculated from measurements of pH, alkalinity, and temperature [32]. Water temperature was controlled at roughly 26 °C throughout experiment periods. pH was measured by a pH meter (Thermo Scientific, Orion benchtop pH meter). Alkalinity was measured based on a colorimetric test using adipic acid and sodium dodecyl sulfate; alkalinity was quantified photometrically at a wavelength of 570 nm.

2.5. Mass balance model development

Mass balance models were developed to describe the dynamic behaviors of gas-phase NCl_3 and CO_2 in indoor pool facilities, to support interpretation of the field measurements at the indoor aquatic center, and to inform strategies for controlling gas-phase concentrations of NCl_3 and CO_2. The models were based on three major assumptions.

1. Two-film theory was used to simulate the net mass-transfer rate of volatile compounds from the liquid-phase to the gas-phase. Two-film theory assumes that net transport is limited by diffusive transport across a thin boundary layer on the liquid side of the gas:liquid interface, a similar layer on the gas side of the interface, or both [33]. This assumption is mechanistically plausible, but represents a simplification of the actual mechanics of transfer.
2. The air space is well-mixed in the studied pool facility. This assumption is not likely to be strictly correct; however, measurements of its dynamics at the studied pool facility indicated similar dynamic behavior of volatile compounds among relatively distant sampling locations, thereby supporting the validity of this assumption [29] (see Figs. SI–4). Mass balance models for characterizing the dynamics of volatile compounds in indoor air often treat the air space as well-mixed [34–36].
3. The composition of water within the actively-mixed layer of water in the pool (the top 30–50 cm) is spatially uniform (*i.e.*, well-mixed). Mechanical mixing by swimmers is largely confined to this layer. Also, net transfer from the liquid-phase to the gas-phase will involve volatile chemicals that are present within this upper layer of the water column within a pool. All water samples were collected from this top layer.

The fundamental equation that was used to define the model for volatile compounds that originate only in the pool water (*e.g.*, NCl_3) is presented below as equation (1). This model is based on principles of mass conservation (*i.e.*, mass balance), with a control region of the (well-mixed) indoor air space above a pool. A schematic illustration of control region and relevant parameters of the balance model is presented in Fig. 1.

$$\forall_g \frac{dC_g}{dt} = Q_g C_{g,in} - Q_g C_g + \Phi_B + \sum_{i=1}^{n} \Phi_{S,i} \tag{1}$$

Where,

$\forall_g$ (m^3) = volume of gas-phase (well-mixed air volume in indoor pool facility)
C_g (mg/m^3) = concentration of volatile compound in the control region, and leaving the control region
t (hr) = time
Q_g (m^3/hr) = volumetric flow rate of outdoor air into (and out of) the control region
$C_{g,in}$ (mg/m^3) = concentration of volatile compound in outdoor air entering the control region
Φ_B (mg/hr) = (net) rate of mass transfer of volatile compound from liquid→gas under baseline conditions
$\Phi_{S,i}$ (mg/hr) = (net) rate of mass transfer of volatile compound from liquid→gas attributable to ith swimmer
n = number of swimmers.

Note that unit conversions are not included explicitly in the model equation or in other equations presented herein, but are implied in the use of these models.

The product on the left-hand side of equation (1) describes the time rate-of change of the mass of a volatile compound in the control region. Volatile DBPs are all assumed to be generated in water exclusively; it is assumed that no other sources of these compounds exist in the system. Schematically, reactions between precursors (P) that are introduced by swimmers and free chlorine are shown in Fig. 1. At present, it is not possible to accurately simulate DBP formation/degradation dynamics in pool water because the kinetics and mechanisms of many of the participating reactions are complex and incompletely defined. However, analytical methods are available to measure the liquid-phase concentrations of some volatile DBPs in pool water.

Under baseline conditions (*i.e.*, when the pool facility is closed and water circulation/mixing are entirely attributable to water recirculation through the treatment system), net liquid→gas transfer of volatile compounds takes place at a rate of Φ_B; this baseline rate of mass transport can be related to other aspects of system behavior through

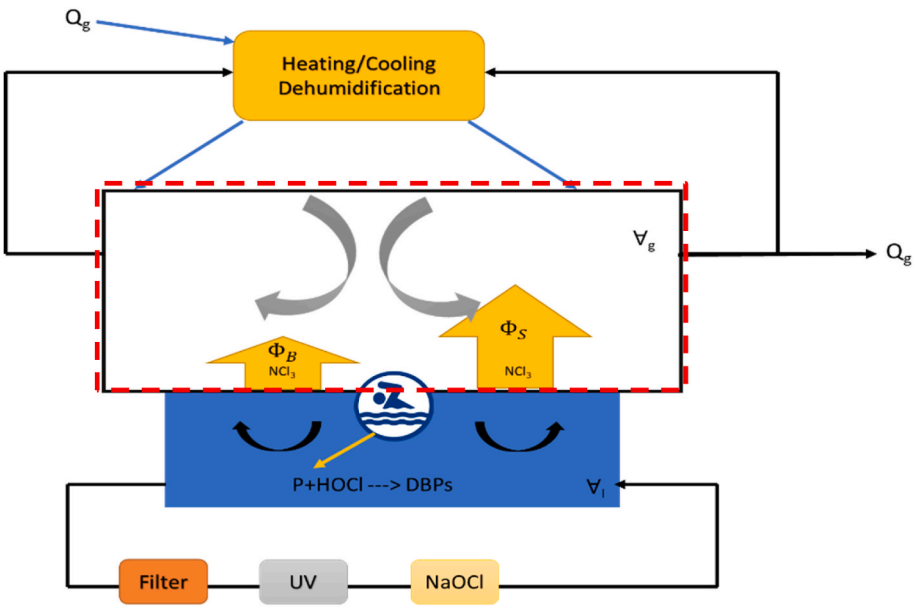

Fig. 1. Schematic illustration of control region and relevant parameters of mass balance model for gas-phase NCl_3. Red dashed line represents the control region, which was assumed to be well-mixed. P represents precursors to DBP formation; HOCl represents hypochlorous acid, the form of free chlorine that is generally most responsible for DBP formation. (For interpretation of the references to color in this figure legend, the reader is referred to the Web version of this article.)
Φ_B: (net) rate of mass transfer of NCl_3 from liquid→gas under baseline conditions.
Φ_S: (net) rate of mass transfer of NCl_3 from liquid→gas attributable to swimmer.
C_g: concentration of NCl_3 in control region and leaving the control region.
Q_g: volumetric flow rate of air into (and out of) the control region.
$\forall_g$: volume of gas-phase in the control region.
$\forall_l$: volume of liquid-phase.

two-film theory. The contribution of this process to IAQ dynamics is described by the third term on the right-side of the governing equation.

Each swimmer is assumed to contribute to net liquid→gas transfer independently at a rate of $\Phi_{S,i}$. The overall rate of net liquid→gas transfer attributable to swimmers is defined as the sum of their individual contributions and each swimmer is assumed to contribute equally to this process. Therefore, if there are n swimmers in the water, the net rate of liquid→gas transfer due to these swimmers is defined by the sum: $\sum_{i=1}^{n}\Phi_{S,i}$ as described by the fourth term in the right-side of the governing equation.

For the specific case of NCl_3, it was assumed that $C_{g,in} = 0$, because outdoor air that is brought into the studied systems was assumed to be 'clean' in terms of gas-phase NCl_3. Two-film theory was used to calculate Φ_B and $\Phi_{S,i}$ by multiplying the flux terms by an appropriate gas:liquid interfacial area. For the baseline condition, the relevant area was the total surface area of the studied pool. Φ_B was calculated as shown in equation (2).

$$\Phi_B = K_l A\left(C_l - C_l^*\right) \tag{2}$$

Where,

K_l (m/hr) = mass-transfer coefficient based on liquid-phase measurements
A (m^2) = total surface area of the swimming pool
C_l (mg/L) = liquid-phase concentration of volatile compound (NCl_3)
C_l^* (mg/L) = liquid-phase concentration of volatile compound (NCl_3) that would be in equilibrium with the gas phase.

When swimmers are present in the pool, each swimmer will impart mechanical mixing energy on the water (and air) in the immediate vicinity of the gas:liquid interface. That mixing energy will promote transfer of volatile compounds across the air:water interface from an area surrounding the swimmer. $\Phi_{S,i}$ was calculated as described in equation (3).

$$\Phi_{S,i} = K_{l,i}A_i\left(C_l - C_l^*\right) \tag{3}$$

Where,

$K_{l,i}$ (m/hr) = overall mass-transfer coefficient based on liquid-phase measurements for the ith swimmer
A_i (m^2) = area disturbed by the ith swimmer.

When applying equations (2) and (3), it was assumed that the liquid-phase concentration of the volatile compound that would be in equilibrium with the gas-phase was negligibly small as compared with C_l and could be ignored. This assumption was based on the fact that measured gas-phase concentrations of volatile DBPs are typically about 1% of their respective equilibrium values [28]. This means that $C_l \gg C_l^*$ for most volatile DBPs in indoor pool facilities, including NCl_3. Therefore, the net mass-transfer caused by a group of n swimmers can be expressed as equation (4).

$$\Phi_S = \sum_{i=1}^{n}\Phi_{S,i} = \sum_{i=1}^{n}K_{l,i}A_iC_l \tag{4}$$

A similar simplification can be applied to equation (2) for calculation of baseline net liquid→gas transfer.

At present, it is impractical to develop an estimate of $K_{l,i}$ for each swimmer. Similarly, it was not possible to accurately measure A_i for each swimmer, independently. As an alternative to estimating these parameters independently for each swimmer, calculations were based on the summation of the product $K_{l,i}A_i$. As such, equation (4) was transformed to equation (5):

$$\sum_{i=1}^{n}K_{l,i}A_iC_l = nK_l^{'}C_l \tag{5}$$

Where,

n: number of swimmers.
$K_l^{'}$ (m^3/hr) = effective mass transfer coefficient (equal to $\sum_{i=1}^{n}K_{l,i}A_i$).

Based on the assumptions described above, the mass balance model for NCl_3 was simplified, as shown in equation (6).

$$\forall_g\frac{dC_g}{dt} = -Q_gC_g + K_lAC_l + nK^{'}C_l \tag{6}$$

A similar approach was used to develop a mass balance model for CO_2. However, the assumption of negligible equilibrium liquid-phase CO_2 was not applicable for the CO_2 model. Other modifications were required because CO_2 is present in the atmosphere naturally; therefore, ambient CO_2 is brought into a pool facility by its mechanical ventilation

system. Also, humans exhale CO_2. Respiration/emission rates of CO_2 for swimmers are also likely to differ from lifeguards, pool workers, and spectators (*i.e.*, non-swimmers). Extra terms were added to the general governing equation to account for gas-phase CO_2 dynamics, as shown in equation (7).

$$\forall_g \frac{dC_g}{dt} = Q_g C_{g,in} - Q_g C_g + K_l A(C_l - C_l^*) + n \bullet K'(C_l - C_l^*) + n \bullet emCO_2' + N \bullet emCO_2 \tag{7}$$

Where,

$C_{g,in}$ (mg/m^3) = concentration of gas-phase CO_2 in outdoor air entering the air space.
C_l^* (mg/L) = equilibrium concentration of liquid-phase CO_2.
n = number of swimmers.
$emCO_2'$ (mg/person·hr) = per person CO_2 emission rate by swimmers.
N = number of non-swimmers.
$emCO_2$ (mg/person·hr) = per person CO_2 emission rate by non-swimmers.

Equations (6) and (7) were applied under the assumption that liquid-phase concentrations of NCl_3 and CO_2 changed linearly (with time) between measured values from pool water samples.

As described previously, CO_2, which forms carbonic acid (H_2CO_3) upon contact with water, was used for pH control in the facility that was the target of these measurements and simulations; this is a common practice in swimming pools. At present, it is not possible to accurately simulate the dynamics of liquid-phase CO_2 concentrations in pools; however, it was possible to estimate liquid-phase CO_2 concentration based on measurements of pH and alkalinity.

2.6. Estimation of parameters

The parameters included in equations (6) and (7) can be measured or estimated. $\forall_g$ was estimated from building drawings, based on the physical dimensions of the air space. Q_g was calculated from measured air velocity as a function of damper opening setting and the cross-sectional dimensions of the inlet duct for studied pool facility. Specifically, for each of the five air handling units at the facility, measurements of air velocity were conducted for each of three damper openings (quantified as percentage of completely open) using a pitot tube. Those measurements involved a grid of air velocity measurements that spanned the cross-section of each duct in which measurements were collected. For each damper setting, the volumetric flow rate of air was calculated as the product of the average of air velocity measurements and the cross-sectional area of the duct. The relationship between volumetric flow rate and damper setting was fit with a quadratic function for each air handler (see Figs. SI–6). Damper opening settings are monitored in real-time at this facility, thereby allowing translation of these measurements to real-time estimates of Q_g.

Gas-phase NCl_3 was measured by the NEMo devices, while liquid-phase NCl_3 was quantified by MIMS. Surface area was calculated based on the measured dimensions of the pool surface. The number of swimmers was recorded at the top of each hour during each sampling period. For equation (6), after dividing both sides of the equation by $\forall_g$, the governing equation can be rearranged as equation (8).

$$\frac{dC_g}{dt} + \frac{Q_g}{\forall_g} C_g = K_l \frac{A}{\forall_g} C_l + \frac{n}{\forall_g} K' C_l \tag{8}$$

Equation (8) can be presented in finite difference form as equation (9) below.

$$\Delta C_g = \frac{\Delta t}{\forall_g}(-Q_g C_g) + \frac{\Delta t}{\forall_g}(K_l A C_l) + \frac{\Delta t}{\forall_g}(nK' C_l) \tag{9}$$

At steady-state $\left(\frac{dC_g}{dt} = 0\right)$, with no swimmers in the pool ($n = 0$), equation (8) will reduce to equation (10).

$$\frac{Q_g}{\forall_g} C_{g,ss} = K_l \frac{A}{\forall_g} C_{l,ss} \tag{10}$$

Where,

$C_{g,ss}$ (mg/m^3) = steady-state concentration of NCl_3 in the gas phase (concentration when no swimmers were present in the pool).
$C_{l,ss}$ (mg/L) = steady-state concentration of NCl_3 in the liquid phase (concentration when no swimmers were present in the pool).

If steady-state concentrations in both phases are achieved, such as in the early morning after an extend period of no use of the pool, it is then possible to rearrange equation (10) to develop an estimate of the value of K_l, as described by equation (11).

$$K_l = \frac{Q_g \bullet C_{g,SS}}{A \bullet C_{l,SS}} \tag{11}$$

The only remaining unresolved term in equation (6) was K'. Equation (9) describes the incremental changes in C_g that took place in each time step of a monitoring period. By extension, this information can be used to simulate the time-course behavior of C_g for a monitoring period:

$$C_g(t + \Delta t) = C_g(t) + \Delta C_g \tag{12}$$

A regression model was used to estimate K' by least-squares fitting of equation (12) to the time-course measurements of gas-phase NCl_3 concentration. It is important to reiterate that the liquid-phase NCl_3 concentration used in the simulations was estimated by linear interpolation between measured values of liquid-phase NCl_3 concentrations. This approach was applied because concentrations of gas-phase NCl_3 were reported every 10 min during the entire sampling periods, yet water samples were collected and analyzed approximately every 2 h when pool facility was open to public; water samples were not collected or analyzed when the pool facility was closed. This process represents a source of error in application of the model.

For equation (7), many of the input parameters were also measurable, including $\forall_g$, Q_g, C_l, n and N. At steady-state, with no people in the pool, equation (7) will reduce to equation (13).

$$Q_g(C_{g,ss} - C_{g,in}) = K_l A(C_{l,ss} - C_l^*) \tag{13}$$

Where,

$C_{g,ss}$ (mg/m^3) = steady-state concentration of CO_2 in the gas phase (concentration when no people were present in the pool facility).
$C_{g,in}$ (mg/L) = concentration of CO_2 in the air that is brought into the pool facility.

This concentration was assumed to be equal to the value reported at the Mauna Loa Observatory at the time of these experiments (410 ppm$_v$), which was converted to mass concentration based on the ideal gas law (T = 25 °C). Gas-phase measurements of CO_2 concentration from the Mauna Loa Observatory were assumed to be representative of the Northern Hemisphere. Coincidentally, measurements of ambient CO_2 concentration in the vicinity of the pool facility were conducted for the period that spanned the experiments reported herein. Those measurements were conducted using the LI-830 CO_2 gas analyzer described previously; they indicated a mean concentration of 410.7 ppm$_v$, with a standard deviation of 18.1 ppm$_v$.

$C_{l,ss}$ (mg/L) = steady-state concentration of CO_2 in the liquid-phase (concentration when no people were present in the pool facility).
C_l^* (mg/L) = equilibrium concentration of CO_2 in the liquid-phase (concentration when no people were present in the pool facility) calculated by application of Henry's law to measured values of CO_2 concentration in air above the pool.

Algebraic rearrangement of equation (13) yields equation (14), which was used to estimate the value of K_l for CO_2.

$$K_l = \frac{Q_g\left(C_{g,ss} - C_{g,in}\right)}{A\left(C_{l,ss} - C_l^*\right)} \tag{14}$$

The term $emCO_2$ was calculated based on reported respiration rates for humans. This calculation was based on several reported values, as illustrated in equation (15). First, humans exhale CO_2 at a concentration of ~4–5% in each breath [37]. Tidal volume represents the volume of air that moves in and out of the lungs with each respiratory cycle. Typical tidal volumes for healthy adult males at rest are roughly 500 mL and approximately 400 mL for healthy adult females [38]. The typical breathing frequency in normal humans is within the range of 10–20 breaths per minute [39]. Thus, $emCO_2$ was calculated as follows:

$$emCO_2 = 450\,\frac{mL}{breath} \times 4.5\% \times 15\,\frac{breath}{minute} = 304\,\frac{mL}{minute} = 18,240\,\frac{mL}{hour} = 32,600\,\frac{mg}{hour} \tag{15}$$

For each of the terms in equation (15) (tidal volume, CO_2 concentration, breathing frequency), a mean value was applied. In addition, these values were assumed to apply generally to all non-swimmers who were present in the facility. The selection of mean values was intended to provide an estimate of the CO_2 emission rate for the non-swimmers that were present in the facility, but also represents a source of error in application of the CO_2 model.

For $emCO_2'$, the respiratory pattern of swimmers was characterized by the tidal volume associated with spontaneous breathing exercise [40]. Measurements of breathing frequency during all-out freestyle, backstroke, or breaststroke swimming in trained swimmers have been reported to be between 39 and 57 breaths per minute and reports of tidal volume have ranged between 1.43 and 3.54 L [40–44]. Thus, $emCO_2'$, was calculated as illustrated in equation (16):

$$emCO_2' = 2000\,\frac{mL}{breath} \times 4.5\% \times 48\,\frac{breath}{minute} = 4320\,\frac{mL}{minute} = 324,000\,\frac{mL}{hour} = 470,000\,\frac{mg}{hour} \tag{16}$$

For comparison, estimates of the CO_2 mass emission rate were developed for non-swimmers and swimmers using a model that accounts for sex, age, body mass, and metabolic rate [45]. For males and females in the age group 21–30, their model predicts CO_2 emission rates of 28, 000 mg/h and 22,000 mg/h respectively at a resting metabolic rate (1.0 met). For a metabolic rate of 20 mets, a plausible value for adult, elite-level swimmers, the CO_2 emission rates for these same groups were calculated as 560,000 mg/h and 440,000 mg/h, respectively. These values are similar to those described above and used in the modeling effort described herein.

2.7. Model fitting processes

Estimates of mass transfer coefficients for NCl_3 at the studied pool were developed by fitting of the mass balance model to data from experiments A and B in a two-step process. First, the data from the overnight periods (*i.e.*, periods of no swimmer activity) were used to identify a steady-state gas-phase NCl_3 concentration; these data were used to estimate a value of K_l. An estimate of K' was then developed by identifying the value that yielded the minimum value of residual sum of the square (RSS) errors of ([measured gas-phase NCl_3 concentration – model gas-phase NCl_3 concentration] [2]) based on equation (6). As described above, linear interpolation was used to estimate liquid-phase NCl_3 concentrations at times between liquid-phase analyses; this approach was applied because liquid-phase NCl_3 concentration was measured less frequently than the gas-phase NCl_3 concentration. Similarly, the number of swimmers in the pool was manually counted only at the top of the hour, while the pool was open; for purposes of these simulations, the number of swimmers in the pool was assumed to be constant for each 1-h period.

Data from experiments B and C at the studied pool were used to develop the CO_2 mass balance model. As described previously, outdoor air flow rate into the system was estimated from recorded measurements of damper settings for each of the five air handling units in the facility. Linear interpolation of these damper settings was used to estimate real-time air flow rate for experiment C; this interpolation approach was applied because gas-phase CO_2 concentration was recorded every 30 s by the LI-COR CO_2 analyzer and air flow rate was reported every 5 min. Similarly, the number of swimmers in the pool was manually counted only at the top of the hour; for purposes of these simulations, the number of swimmers in the pool was assumed to be constant for each 1-h period. Fitting of the model followed the same process as described above for the NCl_3 model.

3. Results and discussion

3.1. Time-course monitoring of NCl_3 and CO_2 in an indoor aquatic center

During experiment A, trends of liquid-phase NCl_3 behavior were observed such that the concentrations generally increased through the day, during periods of heavy swimmer activity (see Fig. 2). A sharp decrease of liquid-phase NCl_3 concentration was noted for the first measurements of each day, as compared to the last measurement of the preceding day. The factors that contributed to this behavior could include recirculation of pool water during the night, resulting in mixing of near-surface water and water from deeper locations during the overnight period. Also, input of NCl_3 precursors by swimmers during operating hours would promote increases in the liquid-phase NCl_3 concentration. During experiment B, liquid-phase NCl_3 trended upward during the competition and decreased overnight, as shown in Fig. 3. The factors that contributed this behavior are likely to have included introduction of NCl_3 precursors into the pool by the swimmers, thereby promoting NCl_3 formation. The rate of formation was apparently faster than the rates of decay and liquid to gas transfer.

For experiment A, measurements of gas-phase NCl_3 concentration were close to zero during the period from midnight to early morning of 7 March and 8 March, as illustrated in Fig. 2. The measurements presented in Fig. 2 illustrate NCl_3 dynamics under conditions of low swimmer numbers. For these conditions, the concentration of gas-phase NCl_3 was consistently low, as compared with the guideline values that have been established for NCl_3 (see discussion below).

In contrast, relatively high gas-phase NCl_3 concentrations were often observed when large numbers of swimmers were present in the pool, such as when more than 100 youth swimmers were in the pool warming up prior to each competition session in experiment B (see Fig. 3). Gas-phase NCl_3 concentrations in this experiment reached as high as 800 μg/m^3 under crowded conditions. Measured concentrations of gas-phase NCl_3 gradually decreased after the warm-up period. Outside of the warm-up period, the concentrations of gas-phase NCl_3 were typically below 400 μg/m^3. During the overnight period when no people were in the facility, gas-phase NCl_3 was measured consistently around 100 μg/m^3. It appeared that gas-phase NCl_3 approached a steady-state, baseline condition during the overnight period.

Two upper limit values have been recommended for gas-phase NCl_3 concentration in recreational pool facilities: 0.5 mg/m^3 was suggested

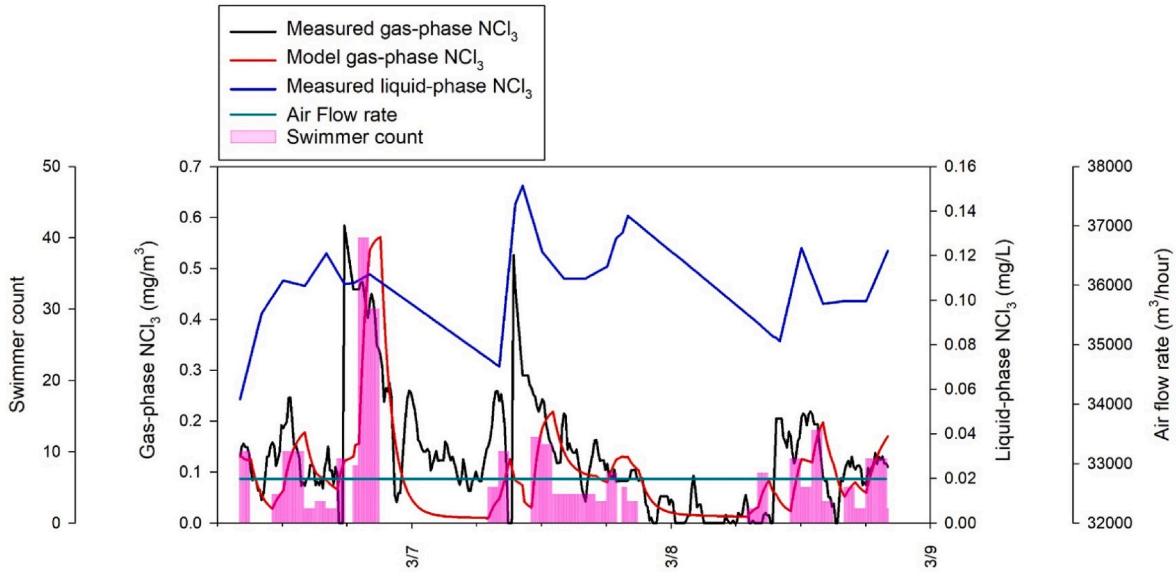

Fig. 2. Time-course measurements of gas-phase NCl_3, liquid-phase NCl_3, and air flow rate for experiment A. Also included are model simulations of the gas-phase NCl_3 concentration. Pink vertical bars represent the number of swimmers in the studied pool. (For interpretation of the references to color in this figure legend, the reader is referred to the Web version of this article.)

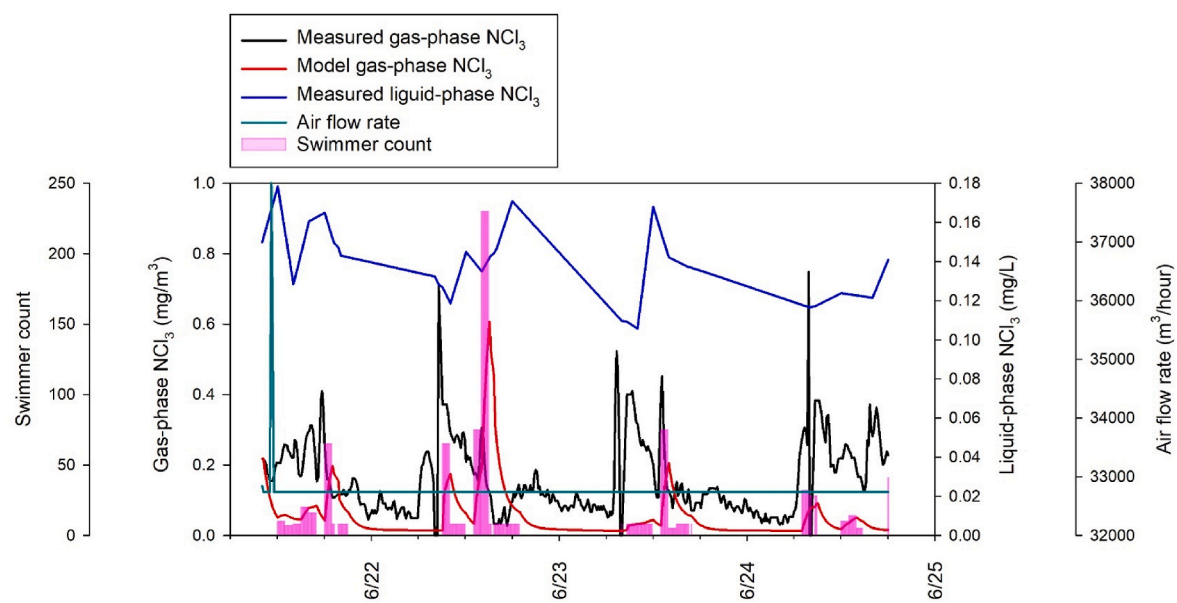

Fig. 3. Time-course measurements of gas-phase NCl_3, liquid-phase NCl_3, and air flow rate for experiment B. Also included are model simulations of gas-phase NCl_3 concentration. Pink vertical bars represent the number of swimmers in the studied pool. (For interpretation of the references to color in this figure legend, the reader is referred to the Web version of this article.)

by the World Health Organization (WHO) [46] as a guideline for safe recreational water environments, while Bernard et al. [47] recommended an upper limit of 0.3 mg/m^3 in swimming pool facilities because at this value an almost immediate increase in lung epithelium permeability was observed, as evidenced by the appearance of surfactant-associated proteins as epithelial permeability markers. Peak gas-phase NCl_3 concentrations were generally observed when large numbers of swimmers were present in the pools. Qualitatively similar behavior has been reported previously [24,26,28,29].

Gas-phase CO_2 was measured as high as 1900 mg/m^3 (1100 ppm$_v$) from the NEMo device during experiment B (Fig. 4). Also, gas-phase CO_2 concentrations showed strong correlations with the number of people in the building during the meet; as many as 500 people were in the building during the meet. After the meet, the CO_2 concentration dropped to around 650 mg/m^3 (360 ppm$_v$) on 6/24.

Gas-phase CO_2 was measured higher than 1500 mg/m^3 (830 ppm$_v$ at 25 °C) from the LI-COR CO_2 analyzer during experiment C (see Fig. 5). In related work, Lee [48] measured gas-phase CO_2 as high as 2800 mg/m^3 (1600 ppm$_v$) during a swimming meet for around 300 swimmers aged 13 to 18 at an indoor pool facility. Also, gas-phase CO_2 was measured as high as 2200 mg/m^3 (1200 ppm$_v$) during a swimming meet for age 14 and under that involved roughly 200 swimmers [49].

For perspective, IAQ criteria often call for CO_2 concentrations to be kept below 1800 mg/m^3 (1000 ppm$_v$) in commercial and other non-industrial settings [45]. A review of published measurements of indoor CO_2 concentrations in commercial and institutional settings

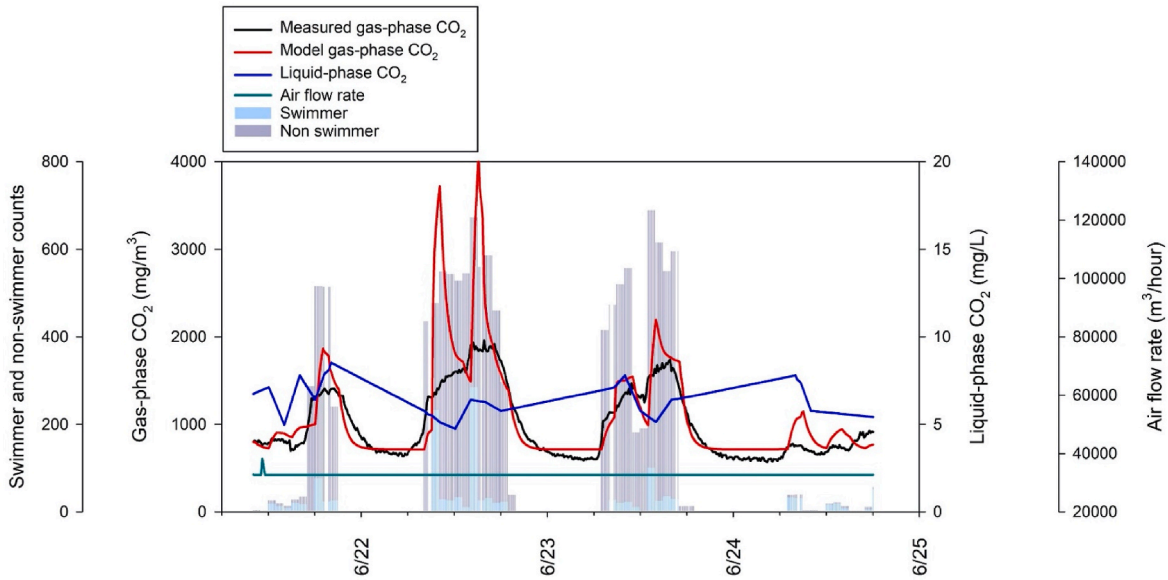

Fig. 4. Time-course monitoring of gas-phase CO_2 and liquid-phase CO_2, and air flow rate for Experiment B. Also included are model simulations of the gas-phase CO_2 concentration. Vertical bars represent the number of swimmers and non-swimmers in the studied pool.

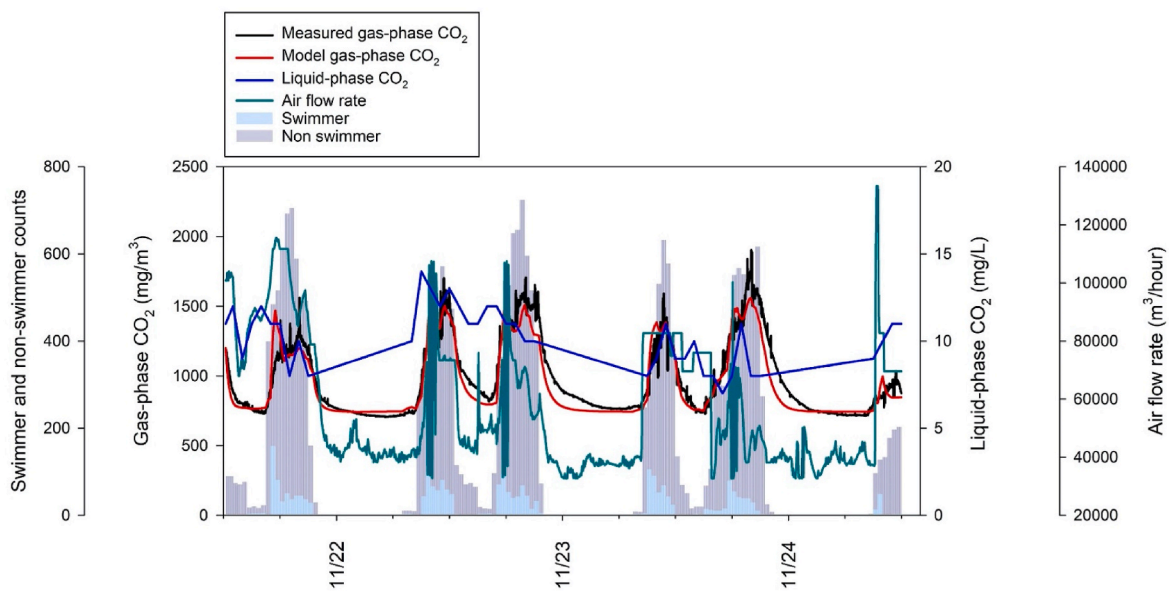

Fig. 5. Time-course monitoring of gas-phase CO_2 (by LI-COR CO_2 analyzer) and liquid-phase CO_2, and air flow rate for Experiment C. Also included are model simulations of the gas-phase CO_2 concentration. Vertical bars represent the number of swimmers and non-swimmers in the studied pool.

indicated measured values ranging from 350 to 3700 ppm_v (630–6700 mg/m^3) [50]. A separate review indicated measured CO_2 concentrations in school classrooms to range from roughly 500–4100 ppm_v (900–9000 mg/m^3) [51]. Interestingly, there is evidence to indicate that adverse human health effects may be associated with CO_2 exposures as low as 1000 ppm_v (1800 mg/m^3) [52]. Given the narrow margins that often separate placement in swimming competitions, especially at the elite level, there may also be motivations for monitoring and control of gas-phase CO_2 in indoor swimming pool facilities. A similar argument can be made for control of gas-phase NCl_3.

The temporal trends in gas-phase CO_2 concentration were similar to the temporal trends of the number of people in the facility during this meet. There were more than 400 people in the facility on several occasions. The majority of people in the facility were actually on the second floor in the spectator area during the swimming meet. The number of people that were outside the pool also included swimmers resting and waiting on the pool deck as well as coaches and meet officials. These people will not affect the dynamic behavior of gas-phase NCl_3 but will affect the dynamic behavior of gas-phase CO_2.

Gas-phase CO_2 was likely transferred from the liquid-phase to the gas-phase by the swimmer's activity. Also, CO_2 was released to the air space of the pool by normal respiratory activities of the swimmers and non-swimmers in attendance during the meet. Thus, the numbers of people in the pool and outside the pool are likely to affect the gas-phase CO_2 concentration. After the meet concluded each day, the CO_2 concentration dropped rapidly and approached the outdoor, ambient concentration.

3.2. NCl_3 mass balance model

Table 1 provides a summary of the values of the best-fit mass transfer coefficients for experiments A and B. The values of K_l multiplied by pool surface area are also shown in Table 1 because mass transfer coefficients are sometimes reported as the product K_lA. The variation of K' between experiments A and B was attributed to differences in the ages of the swimmers from these experiment periods. Specifically, data for experiment A were collected during a period of normal operations, when the majority of swimmers were adult recreational lap swimmers. In contrast, the data from experiment B were collected during a swimming competition for children age 8 and under.

For comparison, reported values of K_l for other air:water systems are as follows. For still ponds and pools that are included in indoor air spaces, reported estimates of K_l ranged from: $1.8\,x\,10^{-4}\frac{m}{hr} \leq K_l \leq 5.63\,x\,10^{-3}\frac{m}{hr}$ [53]. For surface waters that move (*e.g.*, rivers, estuaries), reported estimates are larger. For example, reported estimates of K_l for polychlorinated biphenyl (PCB) air:water exchange in the New York-New Jersey Harbor Estuary were: $0.0013\frac{m}{hr} \leq K_l \leq 0.015\frac{m}{hr}$ [54]. The estimates of K_l in this study are within the range of values reported for this estuary. Schwarzenbach et al. [55]. reported a calculated liquid-phase mass transfer coefficient for NCl_3 of $0.0216\frac{m}{hr}$ for an unused pool, based on the Deacon's boundary layer theory, which is slightly higher than the values observed this study.

The model was applied with the estimated values of mass transfer coefficients to simulate the dynamic behavior of gas-phase NCl_3 concentration for each of the experiments. These simulations were developed using the measured (or interpolated) values liquid-phase NCl_3 concentration, swimmer counts, and air flow rate. The model simulation result for experiment A is illustrated in Fig. 2. During the period of experiment A, the pool was used by recreational lap swimmers, collegiate swim team practice, and for swimming lessons. A source of error in the application of the model for simulations of its dynamics during this period was that only single values of the mass transfer coefficients were applied for each experiment. It is clear that K' will be different when a pool is occupied by swimmers of different ages and different activity levels. Fig. 2 indicates that the timing and magnitude of the simulated peaks of gas-phase NCl_3 concentration were similar to the measured timing and magnitudes of these peaks; however, differences in these values are also clearly evident in the figures.

Swimmer number is a critical factor in governing air quality in indoor pool facilities. Previous experimental measurements and modeling simulations have also supported the importance of the link between swimmer number and IAQ [28,29,56,57]. An important application of this model is for prediction of how often and how long gas-phase NCl_3 will exceed the guideline upper limits of 0.3 mg/m^3 or 0.5 mg/m^3 [46]. Some deviations between model and measurement were evident in these results, but the model predictions were generally similar to measurements from these experiments.

Measurements and simulations of gas-phase NCl_3 dynamic behavior for experiment B are presented in Fig. 3. This experiment was conducted during a swimming meet for 8 and under children in which approximately 350 swimmers participated. Fig. 3 indicates that model predictions of gas-phase NCl_3 were similar to the measured data, but with an apparent lag. As air flow rate in the studied pool was essentially constant and low during this experiment, it is likely that the delay was caused by the low air flow rate for this NCl_3 mass balance simulation. Also, the model predictions of local peak concentrations were not always correct. Further study will be necessary to more completely define the effects of various types of swimmer activity on liquid→gas transfer dynamics. Specifically, it is expected that mechanical mixing of water will vary among activity types, such as competition events, warm-up or warm-down, and the age of the swimmer.

Gas-phase NCl_3 models will be useful as a tool to provide guidance for operators of indoor pools and their HVAC systems, as well as other engineering interventions that may be used to control gas-phase NCl_3 concentration. For example, these models could be useful for prediction of circumstances that will result in the concentration of gas-phase NCl_3 exceeding guidance values. Pool operators could adjust the air handling units to alter the air exchange rate in the pool facility beforehand, thereby maintaining gas-phase NCl_3 concentrations below the target value. Mass balance models for gas-phase NCl_3 can also be integrated with building automation systems to provide real-time control of the outdoor air flow rate.

Two-film theory suggests that liquid-phase concentration of NCl_3 is the driving force for liquid-phase to gas-phase mass transfer. Therefore, it may be possible to mitigate transfer of NCl_3 to air by inclusion of process modifications to reduce liquid-phase NCl_3 concentration. This could be accomplished by inclusion of an air stripping system into the pool water treatment process. With proper installation and operation of such a system, it may be possible to vent volatile compounds directly to outdoor air, rather than to the air space above a pool. This approach recognizes that most of the volatile DBPs, like NCl_3, that are contained in a swimming pool facility will form in the water. Previous studies have demonstrated the effectiveness of air stripping systems for removal of liquid-phase NCl_3 from pool water [56,58]. Such a system could be appropriate to augment mechanical ventilation. However, air stripping systems will consume energy, both by the pumping and ventilation requirements of the system, and by promotion of heat transfer from water [57]. Also, off-gas treatment may be required [59]. Another concern is stripping of desirable chemicals, such as CO_2 which could affect pool water chemistry (*i.e.*, pH control).

Acknowledgement of model limitations is important for proper interpretation of model predictions. Some model limitations are directly attributable to model assumptions. For example, the assumptions of well-mixed air and water layer will not apply strictly to pool facilities. However, during experiment A, three NEMo devices were installed at different locations in the pool facility. The measurements of gas-phase NCl_3 from each sensor indicated that well-mixed conditions were closely approximated, as illustrated in Figs. SI–4. Another limitation of this study was the frequency and location of liquid-phase NCl_3 measurements. In most experiments, liquid-phase NCl_3 was measured once every 2 h from a single location. For application to the mass balance model, linear interpolation was applied to simulate liquid-phase NCl_3 dynamics. In addition, swimmer number was recorded only at the top of the hour, but for the model it was assumed that swimmer count was constant for the entire hour. Another limitation was the assumption of a single value of each mass transfer coefficient being used to describe dynamics during an entire experiment. It is likely that mass transfer behavior will vary with the type of swimming activity, the age and physical strength of the swimmer, and the intensity of their effort. All of these factors will contribute to variability in mass transfer behavior.

3.3. CO_2 mass balance model

The conditions of the experiments and estimated values of K_l and K' are summarized in Table 2. The K' of zero from experiment B indicated that swimmer-induced liquid to gas transfer of CO_2 was negligible (non-detectable) for this event. The main control factors were indicated to be human respiration and input of indoor/outdoor air. The estimate of K' for CO_2 for the experiment C was slightly higher than K' values estimated for NCl_3. The measurements and model gas-phase CO_2 concentrations during experiment B are presented in Fig. 4; as described previously, the swimming competition for experiment B involved children aged 8 and under. The model generally provided a good fit to the data, but it appeared to over-predict two peaks of CO_2 on 6/22. The main reason for the overprediction is believed to be due to the swimmer's exhalation. The model assumed CO_2 exhaled by swimmers would be released entirely into the air space. This assumption will result in an overestimate of the CO_2 contribution by the swimmer's exhalation.

The measurements and model gas-phase CO_2 concentrations at the studied pool for experiment C are presented in Fig. 5. This experiment was conducted during a swimming meet for elite, adult athletes. The graph illustrates a good fit of the model to the data. This suggests that the CO_2 mass balance model may be more appropriate for strong adult swimmers, as opposed to youth swimmers, because liquid→gas transfer is likely to be more important for these stronger swimmers. Both CO_2 mass balance model applications indicated general agreement between measured and modeled CO_2 concentrations; however, clear deviations between measurements and model predictions were also evident.

It is worth noting that the air flow rate illustrated in Fig. 5 is variable, whereas in Figs. 2–4 the air flow rate was essentially constant. Under some conditions, the facility managers choose to operate with a constant air flow rate, while under other conditions (such as a large competition), they choose to operate with automatic control, based on relative humidity.

3.4. Similarities between NCl_3 and CO_2 model temporal predictions

One of the motivations for applying the mass balance model to simulate CO_2 dynamics was to explore the possibility of using gas-phase CO_2 as a surrogate for monitoring gas-phase NCl_3 in swimming pool facilities. Several factors contributed to this idea, including that there are many low-cost (<$100 USD), commercially available CO_2 sensors that could be used to monitor gas-phase CO_2 dynamics in pool facilities. In addition, strong correlations between gas-phase concentrations of NCl_3 and CO_2 have been reported [26]. However, there are important limitations that accompany this approach. Of particular importance is the fact that gas-phase NCl_3 is entirely attributable to transfer from the liquid phase, while gas-phase CO_2 will enter the air space in a pool facility by transfer from the liquid-phase, by respiration of swimmers and non-swimmers in the facility, and from ambient outdoor air.

Measured gas-phase CO_2, modeled gas-phase CO_2, measured gas-phase NCl_3, and modeled gas-phase NCl_3 for experiment B are illustrated in Fig. 6. The timing of the peaks based on measurements and models were consistent, but the magnitudes of the measured peaks diverged from those of the models. This is believed to be largely due to the contribution from swimmer's activity. The NCl_3 mass balance model was developed based on dynamic behavior attributed to swimmers, but the CO_2 mass balance model indicated that liquid→gas transfer of CO_2 promoted by mechanical mixing of youth (age 8 and under) swimmers was negligible ($K' = 0$). It is believed that the mechanical mixing initiated by these young swimmers was insufficient to promote quantifiable liquid→gas transfer of CO_2. This phenomenon may represent a limitation on the use of gas-phase CO_2 as a surrogate for gas-phase NCl_3 in indoor swimming pool facility. However, it is worth noting that the worst IAQ is likely to occur at times when large numbers of adult swimmers are in a pool, so gas-phase CO_2 may still be worth considering as a surrogate for gas-phase NCl_3 for these conditions. To date, only limited sets of gas-phase CO_2 data have been collected and applied to the CO_2 balance model. Additional experiments involving time-course measurements of gas-phase CO_2 and NCl_3 concentrations will be required to further solidify the application of gas-phase CO_2 as surrogate for gas-phase NCl_3.

3.5. NCl_3 model simulations

The mass balance model for gas-phase NCl_3 allows predictions of gas-phase behavior based on input parameters. The model could also be applied to reflect how IAQ could be improved when changes in pool facility operations were made. The mass balance model was used to simulate gas-phase NCl_3 dynamics in the studied pool facility for three hypothetical 24-h periods. Specific input parameters used for these simulations included assumed values of liquid-phase NCl_3, air flow rate, swimmer counts, and NCl_3 liquid-gas mass transfer coefficient. The simulations addressed a scenario involving normal operations, a scenario involving increased ventilation rate, and a scenario involving inclusion of an air stripper. Fig. 7 illustrates the outcomes of these simulations. Fig. 7(A) illustrates behavior under the 'normal' operating scenario, based on assumed liquid-phase NCl_3 concentration of 0.1 mg/L and HVAC system operation at 0.89 hr^{-1}, which are common for this facility. The number of swimmers in the pool as a function of time were

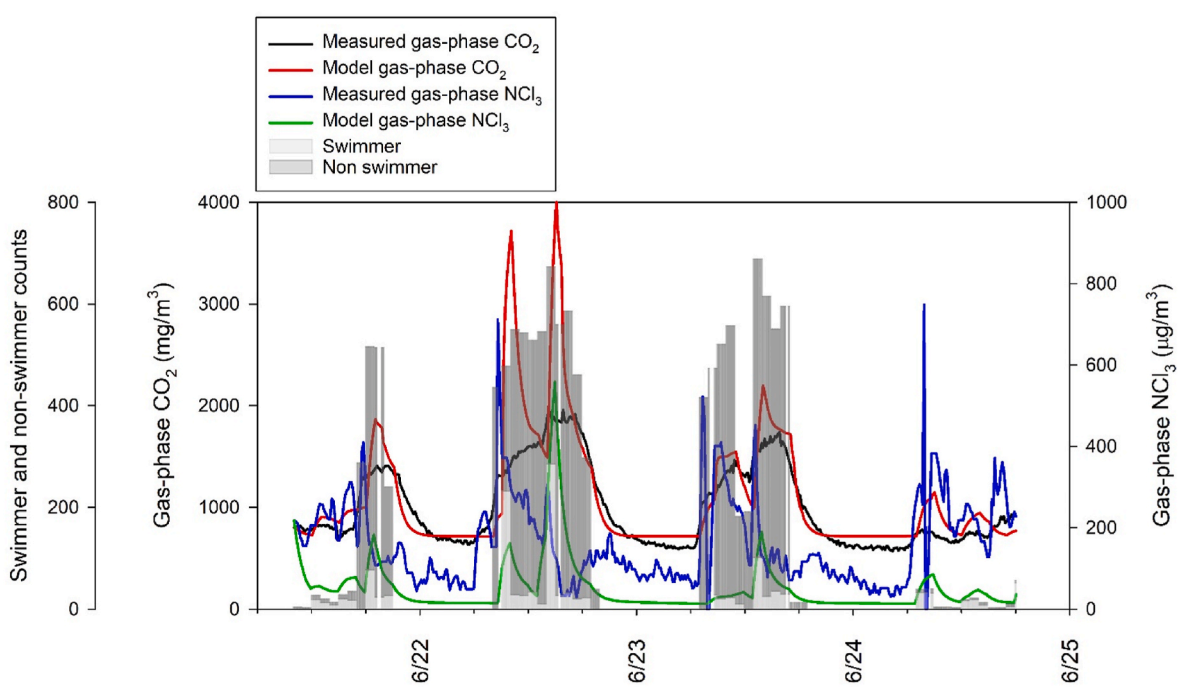

Fig. 6. Time-course monitoring of gas-phase CO_2 and NCl_3 (by NEMo) and model gas-phase CO_2 and NCl_3 in the studied pool during study for experiment B. Black line represents the measured gas-phase CO_2. Red line represents the model gas-phase CO_2. Blue line represents the gas-phase NCl_3 measurement by NEMo device and green line represent the model gas-phase NCl_3 from NEMo device. Vertical bars represent the number of swimmers and non-swimmers in the studied pool. (For interpretation of the references to color in this figure legend, the reader is referred to the Web version of this article.)

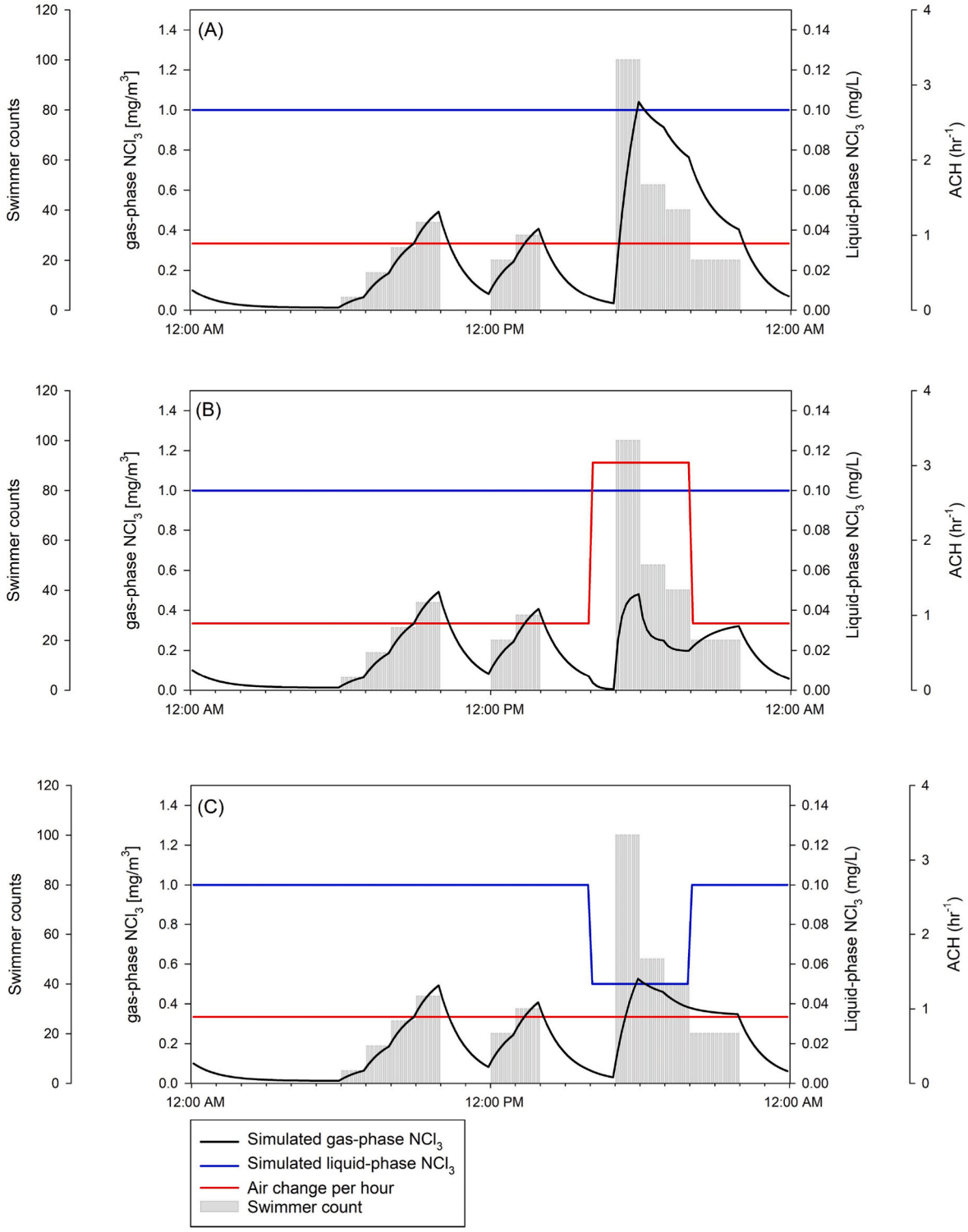

Fig. 7. Simulations of gas-phase NCl_3 dynamics in the studied pool under three different scenarios: (A) normal scenario, (B) air flow rate modified scenario, and (C) air stripping adapted scenario.

selected to be representative of normal pool operation, including a maximum of 100 adult swimmers for the period of 5–7 PM. A peak of gas-phase NCl_3 concentration close to 1.0 mg/m^3 was predicted for this period. This peak is roughly double the guideline gas-phase NCl_3 concentration that has been suggested by WHO and is a condition that would probably lead to coughing and other forms of respiratory distress among swimmers and non-swimmers in the facility.

Fig. 7(B) illustrates predicted behavior for operation of the HVAC system at 3 hr^{-1}, with all other conditions remaining from the first simulation. The increase of ventilation rate was predicted to result in a peak gas-phase NCl_3 concentration of roughly 0.5 mg/m^3, which is consistent with the WHO guideline. A temporary increase in outdoor air flow rate appears to represent a valid control strategy for gas-phase NCl_3 in indoor pools, but will be accompanied by increased costs for heating, cooling, and humidity control during the period of increased air flow rate. Also, this approach assumes that installed HVAC hardware has the

capacity to increase outdoor air flow rate to the value applied in this simulation.

Fig. 7(C) illustrates predicted behavior for the system when the HVAC system was operated at 0.89 hr^{-1}, but with air stripping being initiated immediately before the large number of swimmers entered the pool. This represents a realistic scenario in that events that involve large numbers of swimmers, such as swimming competitions, can be anticipated. For purposes of this simulation, it was assumed that the air stripping device resulted in a reduction of the liquid-phase NCl_3 concentration by 50%, to 0.05 mg/L, during peak hours. It should be noted that air stripping devices can be designed and reliably operated to exceed this level of process efficiency; this value was chosen as a conservative indication of the potential for air stripping to control IAQ in indoor pool facilities. This operating condition resulted in a predicted peak concentration of gas-phase NCl_3 of roughly 0.55 mg/m^3. Therefore, air stripping also appears to represent a valid control strategy for gas-phase NCl_3 in indoor pools. However, operation of an air stripper will involve capital and operating costs. Moreover, air stripping devices will result in net liquid→gas transfer of all volatile chemicals in water, including some compounds that may be beneficial to water quality, such as CO_2. Air stripping will also result in heat transfer, which would need to be compensated for by additional heating of water.

It is important to note that the model was developed based on measurements and simulations of IAQ dynamics in a single competition pool. It is anticipated that the values of the mass transfer coefficients for the swimming populations that were involved in these experiments will translate to other competition facilities. As indicated above, process simulations based on this model could be improved by refinement of swimmer-associated mass transfer coefficients (K') as a function of swimmer age, sex, and physiological capability.

It is likely that differences in IAQ dynamics at pool facilities will be observed in geographic locations where air handling practices or water treatment methods differ from those that applied at the facility in which these tests were conducted. Moreover, it is likely that the potential for net liquid→gas transfer of volatile compounds will be different among pool types. For example, the potential for net liquid→gas transfer of volatile compounds among splash parks and therapy pools is likely to be quite different than those observed in competition or lap swimming pools because the mechanics of mixing behavior near the air:water interface will be quite different among these facilities. Therefore, there is a need to conduct similar experiments in other facilities to allow generalization of this modeling strategy.

The assumption of a well-mixed air space represents another limitation of the model. In practical terms, the well-mixed assumption implies that the temporal patterns of gas-phase composition are similar at all locations within a control region. As describe previously, the air space within the facility where these experiments were conducted closely conformed to the well-mixed assumption [29]. However, some facilities will deviate substantially from a well-mixed condition. When this is the case, the modeling approach described herein will not be appropriate for descriptions of the dynamic behavior of air quality. Under these circumstances, it is likely that accurate predictions of air quality dynamics will require more detailed descriptions of gas-phase fluid dynamics, such as are possible by application of computational fluid dynamics simulations.

4. Conclusions

Time-course measurements of gas-phase NCl_3 indicate that peak concentrations will occur during periods of heavy bather load, especially periods involving adult swimmers. Measurements of the dynamics of gas-phase CO_2 indicate temporal patterns that are similar to those of gas-phase NCl_3, thereby supporting the suggestion that control measures that address gas-phase CO_2 are likely to be effective for control of gas-phase NCl_3 in indoor pool facilities.

Model simulations indicate that peak gas-phase concentrations of volatile compounds, such as NCl_3, can be controlled. Moreover, the NCl_3 model could be used by pool operators and designers of pool facilities to make informed decisions about strategies that could be used to optimize IAQ in pool facilities.

The general framework of the model describe herein is likely to be applicable to other aquatics facilities. However, there is a need to develop a broader set of mass transfer coefficients for liquid→gas transfer of volatile compounds as a function of swimmer age, sex, and physiological capability, as well as for other aquatics activities and for other facility types. Moreover, it would be helpful to evaluate the ability of this model to accurately simulate IAQ dynamics in other geographic settings, where pool operations may differ from the facility that was the subject of this research.

Funding sources

This work was funded by Council for the Model Aquatic Health Code (CMAHC).

CRediT authorship contribution statement

Lester T. Lee: Writing – review & editing, Writing – original draft, Validation, Software, Methodology, Investigation, Formal analysis, Data curation. **Tianren Wu:** Writing – review & editing, Writing – original draft, Validation, Methodology, Investigation, Formal analysis, Data curation, Conceptualization. **Brandon E. Boor:** Writing – review & editing, Writing – original draft, Methodology, Investigation, Formal analysis, Conceptualization. **Ernest R. Blatchley:** Writing – review & editing, Writing – original draft, Validation, Supervision, Software, Resources, Project administration, Methodology, Investigation, Funding acquisition, Formal analysis, Data curation, Conceptualization.

Declaration of competing interest

The authors declare the following financial interests/personal relationships which may be considered as potential competing interests: Ernest R. Blatchley III reports financial support was provided by Council for the Model Aquatic Health Code.

Data availability

Data will be made available on request.

Acknowledgement

The authors are thankful to the Ethera lab for their technical support as making NEMo devices available.

Appendix A. Supplementary data

Supplementary data to this article can be found online at https://doi.org/10.1016/j.buildenv.2023.110088.

References

[1] H. Tanaka, D.R.J. Bassett, E.T. Howley, D.L. Thompson, M. Ashraf, F.L. Rawson, Swimming training lowers the resting blood pressure in individuals with hypertension, J. Hypertens. 15 (6) (1997) 651–657.
[2] Centers of Disease Control and Prevention, Model aquatic health Code: Code language (accessed 2019-01-07), 2018, https://www.cdc.gov/mahc/pdf/2018-MAHC-Code-Clean-508.pdf.
[3] J. Li, E.R. Blatchley III, Volatile disinfection byproduct formation resulting from chlorination of Organic−Nitrogen precursors in swimming pools, Environ. Sci. Technol. 41 (19) (2007) 6732–6739.
[4] E.R. Blatchley III, M. Cheng, Reaction mechanism for chlorination of urea, Environ. Sci. Technol. 44 (22) (2010) 8529–8534.
[5] S. Weng, E.R. Blatchley III, Disinfection by-product dynamics in a chlorinated, indoor swimming pool under conditions of heavy use: national swimming competition, Water Res. 45 (16) (2011) 5241–5248.

[6] L. Lian, Y. E, J. Li, E.R. Blatchley III, Volatile disinfection byproducts resulting from chlorination of uric acid: implications for swimming pools, Environ. Sci. Technol. 48 (6) (2014) 3210–3217.
[7] S. Weng, E.R. Blatchley III, Ultraviolet-induced effects on chloramine and cyanogen chloride formation from chlorination of amino acids, Environ. Sci. Technol. 47 (9) (2013) 4269–4276, https://doi.org/10.1021/es400273w.
[8] S.C. Weng, J. Li, K.V. Wood, H.I. Kenttämaa, P.E. Williams, L.M. Amundson, E. R. Blatchley III, UV-induced effects on chlorination of creatinine, Water Res. 47 (14) (2013) 4948–4956, https://doi.org/10.1016/j.watres.2013.05.034.
[9] E. Yue, H. Bai, L. Lian, J. Li, E.R. Blatchley III, Effect of chloride on the formation of volatile disinfection byproducts in chlorinated swimming pools, Water Res. (2016).
[10] Q. Yang, Y. Guo, J. Xu, X. Wu, B. He, E.R. Blatchley III, J. Li, Photolysis of N-chlorourea and its effect on urea removal in a combined pre-chlorination and UV (254) process, J. Hazard Mater. 411 (2021), 125111, https://doi.org/10.1016/j.jhazmat.2021.125111.
[11] Y. E, Q. Yang, Y. Guo, L. Lian, J. Li, E.R. Blatchley III, CH_3NCl_2 formation from chlorination of carbamate insecticides, Environ. Sci. Technol. 53 (22) (2019) 13098–13106, https://doi.org/10.1021/acs.est.9b03891.
[12] Bernard S. Michel, O. Higuet, S. de Burbure, C. Buchet, J. Hermans, C. Dumont, X. Doyle, I. Afred, C. Lung, Hyperpermeability and asthma prevalence in schoolchildren: unexpected associations with the attendance at indoor chlorinated swimming pools, Occup. Environ. Med. 60 (6) (2003) 385–394.
[13] L. Erdinger, K.P. Kühn, F. Kirsch, R. Feldhues, T. Fröbel, B. Nohynek, T. Gabrio, Pathways of trihalomethane uptake in swimming pools, Int. J. Hyg Environ. Health 207 (6) (2004) 571–575, https://doi.org/10.1078/1438-4639-00329.
[14] M. Hery, G. Hecht, J.M. Gerber, J.C. Gender, G. Hubert, J. Rebuffaud, Exposure to chloramines in the atmosphere of indoor swimming pools, Ann. Occup. Hyg. 39 (1995) 427.
[15] J.H. Jacobs, S. Spaan, G.B.G.J. van Rooy, C. Meliefste, V.A.C. Zaat, J. M. Rooyackers, D. Heederik, Exposure to trichloramine and respiratory symptoms in indoor swimming pool workers, Eur. Respir. J. 29 (4) (2007) 690–698, https://doi.org/10.1183/09031936.00024706.
[16] N. Massin, A.B. Bohadana, P. Wild, M. Héry, J.P. Toamain, G. Hubert, Respiratory symptoms and bronchial responsiveness in lifeguards exposed to nitrogen trichloride in indoor swimming pools, Occup. Environ. Med. 55 (4) (1998) 258–263.
[17] K.M. Thickett, J.S. McCoach, J.M. Gerber, S. Sadhra, P.S. Burge, Occupational asthma caused by chloramines in indoor swimming-pool air, Eur. Respir. J. 19 (5) (2002) 827–832.
[18] R. Sander, Compilation of Henry's Law Constants for Inorganic and Organic Species of Potential Importance in Environmental Chemistry (Version 3), 1999.
[19] M. Zare Afifi, Effects of UV-Based Treatment on Water and Air Chemistry in Chlorinated Indoor Pools, Purdue University, West Lafayette, 2015.
[20] N. Massin, A.B. Bohadana, P. Wild, M. Héry, J.P. Toamain, G. Hubert, Respiratory symptoms and bronchial responsiveness in lifeguards exposed to nitrogen trichloride in indoor swimming pools, Occup. Environ. Med. 55 (4) (1998) 258–263.
[21] J. Parrat, G. Donzé, C. Iseli, D. Perret, C. Tomicic, O. Schenk, Assessment of occupational and public exposure to trichloramine in Swiss indoor swimming pools: a proposal for an occupational exposure limit, Ann. Occup. Hyg. 56 (3) (2012) 264–277.
[22] A.B. Bowen, J.C. Kile, C. Otto, N. Kazerouni, C. Austin, B.C. Blount, H.-N. Wong, M. J. Beach, A.M. Fry, Outbreaks of short-incubation ocular and respiratory illness following exposure to indoor swimming pools, Environ. Health Perspect. 115 (2) (2007) 267–271, https://doi.org/10.1289/ehp.9555.
[23] S.C. Kaydos-Daniels, M.J. Beach, T. Shwe, J. Magri, D. Bixler, Health effects associated with indoor swimming pools: a suspected toxic chloramine exposure, Publ. Health 122 (2) (2008) 195–200, https://doi.org/10.1016/J.PUHE.2007.06.011.
[24] L.T. Lee, E.R. Blatchley III, Long-term monitoring of water and air quality at an indoor pool facility during modifications of water treatment, Water 14 (2022) 335, https://doi.org/10.3390/W14030335. Page 335 2022, 14 (3).
[25] M. Zare Afifi, E.R. Blatchley III, Effects of UV-based treatment on volatile disinfection byproducts in a chlorinated, indoor swimming pool, Water Res. 105 (2016).
[26] M. Zare Afifi, E.R. Blatchley III, Seasonal dynamics of water and air chemistry in an indoor chlorinated swimming pool, Water Res. 68 (2015) 771–783, https://doi.org/10.1016/j.watres.2014.10.037.
[27] B. Lévesque, L. Vézina, D. Gauvin, P. Leroux, Investigation of air quality problems in an indoor swimming pool: a case study, Ann. Occup. Hyg. 59 (8) (2015) 1085–1089.
[28] S. Weng, W.A. Weaver, M. Zare Afifi, T.N. Blatchley, J.S. Cramer, J. Chen, E. R. Blatchley III, Dynamics of gas-phase trichloramine (NCl_3) in chlorinated, indoor swimming pool facilities, Indoor Air 21 (5) (2011) 391–399, https://doi.org/10.1111/j.1600-0668.2011.00710.x.
[29] T. Wu, T. Földes, L.T. Lee, D.N. Wagner, J. Jiang, A. Tasoglou, B.E. Boor, E. R. Blatchley III, Real-time measurements of gas-phase trichloramine (NCl_3) in an indoor aquatic center, Environ. Sci. Technol. 55 (12) (2021) 8097–8107, https://doi.org/10.1021/acs.est.0c07413.
[30] T.B. Nitter, K.v.H. Svendsen, Modelling the concentration of chloroform in the air of a Norwegian swimming pool facility-A repeated measures study, Sci. Total Environ. 664 (2019) 1039–1044, https://doi.org/10.1016/j.scitotenv.2019.02.113.
[31] T.B. Nitter, M.S. Grande, K.V.H. Svendsen, R.B. Jørgensen, S. Carlucci, G. Cao, Can CO2 sensors in the ventilation system of a pool facility help reduce the variability in the trihalomethane concentration observed in indoor air? Environ. Int. 138 (2020), 105665 https://doi.org/10.1016/j.envint.2020.105665.
[32] C.S. Tucker, Carbon dioxide, in: T.L. Wellborn, J.R. MacMillan Jr. (Eds.), For Fish Farmers 84-2, 1984.
[33] W.K. Lewis, W.G. Whitman, Principles of gas absorption, Ind. Eng. Chem. 16 (12) (1924) 1215–1220, https://doi.org/10.1021/ie50180a002.
[34] T. Wu, A. Tasoglou, H. Huber, P.S. Stevens, B.E. Boor, Influence of mechanical ventilation systems and human occupancy on time-resolved source rates of volatile skin oil ozonolysis products in a LEED-certified office building, Environ. Sci. Technol. 55 (24) (2021) 16477–16488, https://doi.org/10.1021/acs.est.1c03112.
[35] X. Tang, P.K. Misztal, W.W. Nazaroff, A.H. Goldstein, Volatile organic compound emissions from humans indoors, Environ. Sci. Technol. 50 (23) (2016) 12686–12694, https://doi.org/10.1021/acs.est.6b04415.
[36] Z. Finewax, D. Pagonis, M.S. Claflin, A. v Handschy, W.L. Brown, O. Jenks, B. A. Nault, D.A. Day, B.M. Lerner, J.L. Jimenez, P.J. Ziemann, J.A. de Gouw, Quantification and source characterization of volatile organic compounds from exercising and application of chlorine-based cleaning products in a university athletic center, Indoor Air 31 (5) (2021) 1323–1339, https://doi.org/10.1111/ina.12781.
[37] J. Taucher, A. Hansel, A. Jordan, W. Lindinger, Analysis of compounds in human breath after ingestion of garlic using proton-transfer-reaction mass Spectrometry, J. Agric. Food Chem. 44 (12) (1996) 3778–3782.
[38] S. Hallett, J.v. Ashurst, Physiology, Tidal Volume, StatPearls, 2019 *[Internet]*.
[39] M.A. Russo, D.M. Santarelli, D. O'Rourke, The physiological effects of slow breathing in the healthy human, Breathe 13 (4) (2017) 298, https://doi.org/10.1183/20734735.009817. LP – 309.
[40] F. Rodríguez, Maximal oxygen uptake and cardiorespiratory response to maximal 400-m free swimming, running and cycling tests in competitive swimmers, J. Sports Med. Phys. Fit. 40 (2000) 87–95.
[41] A. Bonen, B.A. Wilson, M. Yarkony, A.N. Belcastro, Maximal oxygen uptake during free, tethered, and flume swimming, J. Appl. Physiol. Respir. Environ. Exerc. Physiol. 48 (2) (1980) 232–235, https://doi.org/10.1152/jappl.1980.48.2.232.
[42] I. Holmér, A. Lundin, B.O. Eriksson, Maximum oxygen uptake during swimming and running by elite swimmers, J. Appl. Physiol. 36 (6) (1974) 711–714, https://doi.org/10.1152/jappl.1974.36.6.711.
[43] I. Holmér, E.M. Stein, B. Saltin, B. Ekblom, P.O. Astrand, Hemodynamic and respiratory responses compared in swimming and running, J. Appl. Physiol. 37 (1) (1974) 49–54, https://doi.org/10.1152/jappl.1974.37.1.49.
[44] J.R. Magel, J.A. Faulkner, Maximum oxygen uptakes of college swimmers, J. Appl. Physiol. 22 (5) (1967) 929–933, https://doi.org/10.1152/jappl.1967.22.5.929.
[45] A. Persily, L. de Jonge, Carbon dioxide generation rates for building occupants, Indoor Air 27 (5) (2017) 868–879, https://doi.org/10.1111/ina.12383.
[46] Who, Guidelines for Safe Recreational Water Environments; Geneva, vol. 2, 2006.
[47] A. Bernard, S. Carbonnelle, C. de Burbure, O. Michel, M. Nickmilder, Chlorinated pool attendance, atopy, and the risk of asthma during childhood, Environ. Health Perspect. 114 (10) (2006) 1567–1573, https://doi.org/10.1289/ehp.8461.
[48] L.T.C. Lee, Dynamic behavior of water and air chemistry in indoor pool facilities, November 22 (2021), https://doi.org/10.25394/PGS.16695223.v1.
[49] L.T. Lee, Fate and Behavior of Pharmaceuticals and Personal Care Products in Chlorinated Swimming Pools, Purdue University, Thesis, 2016.
[50] O.A. Seppänen, W.J. Fisk, M.J. Mendell, Association of ventilation rates and CO_2 concentrations with health AndOther responses in commercial and institutional buildings, Indoor Air 9 (4) (1999) 226–252, https://doi.org/10.1111/j.1600-0668.1999.00003.x.
[51] L. Chatzidiakou, D. Mumovic, A.J. Summerfield, What do we know about indoor air quality in school classrooms? A critical review of the literature, Intell. Build. Int. 4 (4) (2012) 228–259, https://doi.org/10.1080/17508975.2012.725530.
[52] T.A. Jacobson, J.S. Kler, M.T. Hernke, R.K. Braun, K.C. Meyer, W.E. Funk, Direct human health risks of increased atmospheric carbon dioxide, Nat. Sustain. 2 (8) (2019) 691–701, https://doi.org/10.1038/s41893-019-0323-1.
[53] Z. Guo, N.F. Roache, Overall mass transfer coefficient for pollutant emissions from small water pools under simulated indoor environmental conditions, Ann. Occup. Hyg. 47 (4) (2003) 279–286, https://doi.org/10.1093/annhyg/meg035.
[54] L.A. Totten, P.A. Brunciak, C.L. Gigliotti, J. Dachs, Glenn, E.D. Nelson, S. J. Eisenreich, Dynamic Air−Water exchange of polychlorinated biphenyls in the New York−New Jersey harbor estuary, Environ. Sci. Technol. 35 (19) (2001) 3834–3840, https://doi.org/10.1021/es010791k.
[55] R.P. Schwarzenbach, P.M. Gschwend, D.M. Imboden, Environmental Organic Chemistry, John Wiley & Sons, 2003.
[56] F. Gérardin, M. Héry, Effects of Nitrogen Trichloride Stripping on Air Quality in Indoor Swimming Pools, 2005.
[57] L. Tsamba, O. Correc, A. Couzinet, Chlorination by-products in indoor swimming pools: development of a pilot pool unit and impact of operating parameters, Environ. Int. 137 (2020), 105566, https://doi.org/10.1016/j.envint.2020.105566.
[58] R. Tardif, M. Rodriguez, C. Catto, G. Charest-Tardif, S. Simard, Concentrations of disinfection by-products in swimming pool following modifications of the water treatment process: an exploratory study, J. Environ. Sci. (China) 58 (2017) 163–172, https://doi.org/10.1016/j.jes.2017.05.021.
[59] J.-C. Huang, C. Shang, in: L.K. Wang, Y.-T. Hung, N.K. Shammas (Eds.), Advanced Physicochemical Treatment Processes, Humana Press, Totowa, NJ, 2006, pp. 47–79, https://doi.org/10.1007/978-1-59745-029-4_2.